Microstructure of the spin reorientation transition in second-order approximation of magnetic anisotropy

E. Y. Vedmedenko,[1,2,*] H. P. Oepen,[1] and J. Kirschner[2]
[1]*Institut für Angewandte Physik, Jungiusstr. 11, 20355 Hamburg, Germany*
[2]*Max-Planck-Institut für Mikrostrukturphysik, Weinberg 2, 06120 Halle, Germany*
(Received 13 September 2001; revised manuscript received 16 September 2002; published 4 December 2002)

The microstructure of the magnetization reorientation in second-order perpendicular anisotropy approximation is theoretically studied by means of Monte Carlo simulations. The magnetic structure is investigated as a function of $K_1^{eff}=K_1-E_D$—the difference between first-order anisotropy and demagnetizing energy density—and the second-order anisotropy energy density K_2. For $K_2>0$ the transition from a vertical to in-plane orientation of the magnetization proceeds via the canting of magnetization. The canted phase consists of domains. The domain microstructure establishes the smooth, continuous connection between the vertical domain structure and the vortex structure for in-plane magnetization. For $K_2<0$ a continuous reorientation via a state of coexisting domains with vertical and in-plane magnetization is found. Within this state the size of the vertical and the in-plane domains depends on the ratio of K_1^{eff} and K_2 and changes continuously while the transition proceeds. Both, K_1^{eff} and K_2 determine the width and energy of the domain walls. The broadening and coalescing of domain walls found in first-order anisotropy approximation is prevented by the nonvanishing second-order contribution.

DOI: 10.1103/PhysRevB.66.214401 PACS number(s): 75.70.Kw, 75.70.Ak, 75.60.Ch, 75.40.Mg

Experiments on spin reorientation transition in ultrathin films have revealed that the magnetic microstructure determines to a large extent the magnetic behavior of the system.[1–7] Theoretically, the microstructure of the spin reorientation transition (SRT) has been investigated in first-order approximation of the perpendicular magnetic anisotropy.[8–10] The importance of higher-order anisotropy contributions in the spin reorientation transition has been pointed out,[11–13] and a phenomenological magnetic phase diagram in second-order anisotropy approximation was introduced in 1959.[11] In this approximation only two different kinds of reorientation have been postulated. The reorientation can proceed either through a canting of the magnetization or through a state of coexisting local minima for the in-plane and vertical magnetizations.

The first option is usually quoted as a second-order transition or a continuous reorientation. It is commonly believed that the canted magnetic moments in that, so-called, ''cone state'' are evenly distributed on the perimeter of the base of a cone with no preferred direction of the in-plane components. A possible microstructure of that phase has not yet been considered.

The second kind of transition proceeds via states of ''coexisting phases.'' The reorientation through this path is often classified as a discontinuous or first-order SRT. The classification is due to the assumptions or the models that are made to explain the flip of the moment. In the state of coexisting phases both orientations of the magnetization have local minima. Hence there is a possibility for the magnetization to be oriented along one direction or the other. Two models of occupation are commonly accepted leading to a discontinuous flip, i.e., the ''perfect delay'' and the ''Maxwell'' convention.[14] Initially in both models the magnetization occupies the state of the lowest minimum. In the first model the magnetization is believed to stay in that state until the corresponding minimum of the free energy is completely erased. The second model assumes that the orientation of the magnetization is always determined by the lowest lying energy minimum. A sudden flop appears at the point where both minima have equal depth. Both models have been discussed in the literature for zero temperature. In the common discussion of the discontinuous transition neither the finite temperature nor any microstructure has been taken seriously into account.

This paper focuses on the magnetic microstructure within the spin reorientation, considering anisotropies in the second-order approximation. This is performed by means of computer simulations by a spatially resolved analysis of the magnetization reorientation in the framework of competing dipolar, first- and second-order contributions of the perpendicular anisotropy for a given exchange coupling. For this purpose Monte Carlo (MC) simulations have been performed to find the equilibrium spin configuration at a given temperature. The approach is more general than any previous attempt[8,15] as neither a restriction to one dimension is made nor is a particular domain structure and wall profile assumed. The films are described by an averaged anisotropy. An effect of the layer dependence of the anisotropy on the magnetization orientation is disregarded. The Hamiltonian of the problem includes the exchange, dipolar interactions, and perpendicular anisotropy of the first and second order,

$$\mathcal{H}=-J\sum_{\langle ij\rangle}\mathbf{S}_i\cdot\mathbf{S}_j+\mathbf{D}\sum_{ij}\left(\frac{\mathbf{S}_i\cdot\mathbf{S}_j}{\mathbf{r}_{ij}^3}-3\frac{(\mathbf{S}_i\cdot\mathbf{r}_{ij})(\mathbf{S}_j\cdot\mathbf{r}_{ij})}{\mathbf{r}_{ij}^5}\right)+\mathbf{K}_1\sum_i\sin^2\theta+\mathbf{K}_2\sum_i\sin^4\theta, \quad (1)$$

where J is the exchange coupling constant which is nonzero only for nearest-neighbor spins, D is the dipolar coupling parameter, and $\mathbf{r}_{ij}$ is the vector between sites i and j, θ denotes the angle to the surface normal. The coefficients K_1

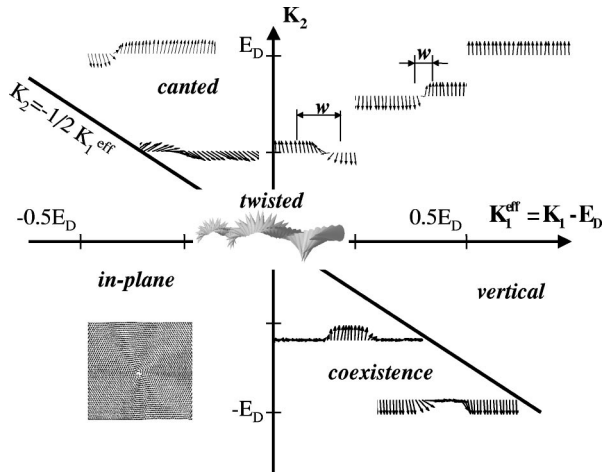

FIG. 1. Micromagnetic phases of a monolayer of classical magnetic moments in the anisotropy space (second-order uniaxial anisotropy approximation) after Ref. 11 and 15. K_1^{eff} is the difference between first-order anisotropy and demagnetizing energy density $K_1^{eff}=K_1-E_D$, and K_2 is the second-order anisotropy density. The lines $K_2=-\frac{1}{2}K_1^{eff}$ and $K_1^{eff}=0$ separate vertical, canted, in-plane, and coexistence phases (see the text). The reorientation transition is characterized by the evolution of magnetic microstructure between vertical and in-plane phases. Please note the different scale on the two axes.

and K_2 are correspondingly the first- and the second-order anisotropy constants. Via scaling the realistic effective values for the ratio of dipolar to exchange interactions can be achieved by considering spin blocks of appropriate size.[16] For the extended MC computations we take a monolayer of classical magnetic moments on a regular, triangular lattice of about 10 000 effective magnetic sites. This corresponds to a surface of an hcp(0001) structure or an fcc(111) structure. The magnetic moment is described by a three-dimensional vector S of unit length. The Monte Carlo procedure is the same as described in previous publications.[10,16] To avoid artificial periodic patterns we use open boundary conditions.

We would like to discuss the results in the appropriate anisotropy space. For the sake of simplicity the diagram is given by K_1^{eff}—the difference between the first-order anisotropy K_1 and the demagnetizing energy density E_D—and the second-order anisotropy energy density K_2 (Fig. 1). Thus K_1^{eff} takes the magnetostatic energy contribution into account. E_D is taken as the magnetostatic energy of an infinite film, i.e., $2\pi M_S^2$. We want, however, to strengthen that in the simulations the magnetostatic energies are calculated exactly while the phase diagram helps to make the presentation of the findings clearer. For positive K_1^{eff} and K_2 a vertical magnetization is favored, while negative values cause an in-plane state [see Eq. (1)].

In the region of ''vertical'' magnetization (Fig. 1), for positive K_1^{eff} and $K_2>-\frac{1}{2}K_1^{eff}$, we find the following microstructure. For large K_1^{eff} the vertically magnetized domains are very large. With K_1^{eff} decreasing more and more vertically magnetized domains appear, i.e., the domain size shrinks. Simultaneously the domain walls become broader. This result is similar to the findings in first-order anisotropy approximation.[8,10] Domains of that size have been experimentally observed close to the reorientation transition in annealed Co/Au(111) films.[3–5] If K_2 is large the domain size and the domain wall width are mainly determined by K_2. The trend is that the stronger the second-order anisotropy the narrower are domain walls and the larger the domains. In the close vicinity of $K_1^{eff}=0$ with nonvanishing K_2 the wall width is finite in contrast to the infinite sinuslike profile of the magnetization in the first-order anisotropy approximation. This means that K_2 substitutes for K_1 in the definitions of the wall width and energy which were already put forward in a theoretical paper[17] some time ago. For $K_1^{eff}=0$ and $K_2=0$ the microstructure consists of moments of spatially varying orientation. The arrangement of the magnetic moments is illustrated in the central inset of the Fig. 1. The magnetization rotates in a helicoidal form along all three principal axes. The structure that forms is called the twisted phase. At this particular point the magnetic moments are evenly oriented in all directions which is characteristic of the twisted configuration.[10]

For negative K_1^{eff} and $K_2<-\frac{1}{2}K_1^{eff}$ (the ''*in-plane*'' region in Fig. 1), the vertical magnetization vanishes and a complete in-plane orientation of the magnetic moments exists. To minimize the magnetostatic energy vortex structures form as the magnetic anisotropy in the film plane is set to zero. In the ''in-plane'' region K_2 has only a minor influence on the microstructure compared to the former situation with $K_1^{eff}>0$.

In the following we will discuss situations where the microstructure is strongly dominated by the interplay of K_1^{eff} and K_2. At first for $K_1^{eff}<0$ and $K_2>-\frac{1}{2}K_1^{eff}$ (inset *canted* in Fig. 1) the negative K_1^{eff} competes with the positive K_2. The energy minimization requires a canting of the magnetization to the film normal.[11–13,15,18] In fact we find a canting of magnetic moments in the simulation (Fig. 1). The vertical component of magnetization changes continuously from 1 at $K_1^{eff}=0$ to zero at $K_2\approx-\frac{1}{2}K_1^{eff}$. In the literature this phase is called the ''cone state'' as it is generally assumed that the canted magnetic moments are distributed uniformly on a perimeter of the base of a cone. We find, however, that the canted magnetic moments form domains with in-plane components oriented along the principal directions in the lattice plane although the in-plane anisotropy was set to zero. This is at variance with Ref. 19, where no preferred direction of the in-plane components was found. The principal axes of the triangular lattice become the in-plane easy axes of magnetization due to dipolar interaction.[20] We may conclude that in the canted phase the ferromagnetic system is already affected by negligibly small in-plane anisotropies. The in-plane anisotropy causes the appearance of domains with magnetization components along distinct in-plane directions. A top view of the domain structure in the canted regime is presented in Fig. 2. In Fig. 2(a) different shades of gray represent different orientations of the magnetic moments in the film plane. In Fig. 2(b) the different shades of gray give the up and down components of the magnetization. The frequency distribution of the in-plane component of magnetization in the down-canted domains is given in Fig. 2(c). This

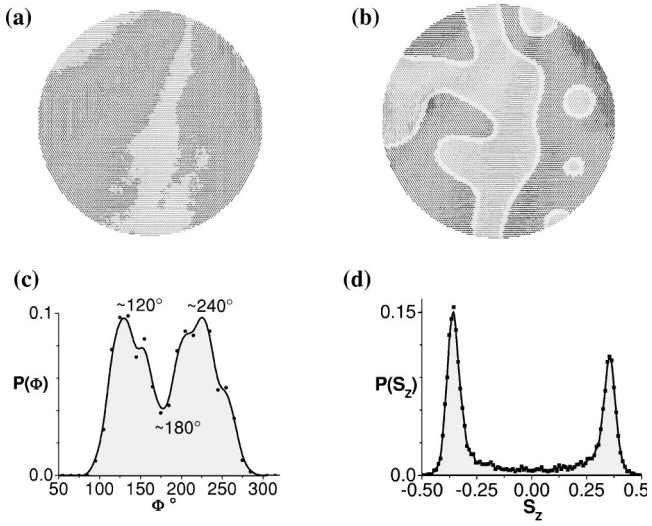

FIG. 2. Top view of the magnetic microstructure in the canted phase for $K_1^{eff}=-0.4E_D$, $K_2=0.65E_D$, and $k_BT/J=0.05$. (a) A top view of the microstructure. In this image the in-plane component of magnetization is coded in gray. Light-gray color gives the part of the sample with an in-plane component pointing mainly to left or right in the plane of drawing (azimuthal orientation of 0° or 180°). The dark-gray color indicates the regions having the in-plane components of magnetization at the angle of 60° or 240° to the horizontal within the plane of drawing. (b) Out-of-plane components of magnetization in the same sample. Dark and light-gray arrows represent canted-down and canted-up domains correspondingly. (c) The frequency distribution of the in-plane component of magnetization. The abscissa gives the angle of the magnetization to the horizontal within the plane of drawing. (d) The frequency distribution of the out-of-plane component of the magnetization. The abscissa gives the component of the magnetization along the normal.

demonstrates that two main in-plane orientations of the magnetization (around 240° and 120°) appear. For the vertical component the frequency histogram [Fig. 2(d)] reveals that the angle to the film normal is identical for all moments in the domains. The angle is equal to the value one obtains from the analytical treatment in case of

$$0 \leqslant -\frac{1}{2}\frac{K_1^{eff}}{K_2} \leqslant 1,$$

i.e.,

$$\theta_M \approx \arcsin\sqrt{-\frac{K_1^{eff}}{K_2}}.$$

The small amount of deviating orientations is found in the domain walls. A three-dimensional representation of the magnetic moments is given in Fig. 3.

We also find that in the canted state the domain size increases with increasing K_2 for a given K_1^{eff}. The width of the domain walls depends on both K_1^{eff} and K_2. The walls become broader with the ratio K_2/K_1^{eff} approaching $-1/2$. The broadening of domain walls causes a slower rotation of magnetization within the wall. As the canting angle is also

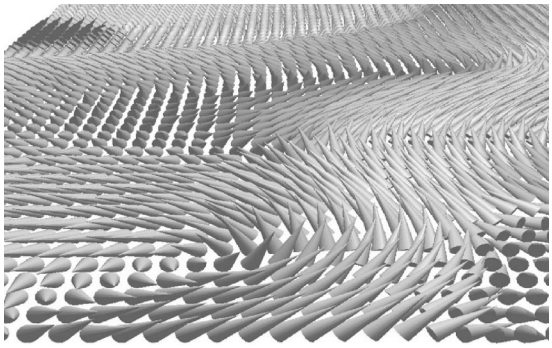

FIG. 3. Perspective view of the canted spin structure for $K_1^{eff}=-0.4E_D$, $K_2=0.65E_D$, and $k_BT/J=0.05$. For clarity only one row out of two and one moment out of two in the row are drawn as cones.

increasing with K_2/K_1^{eff} approaching $-1/2$ the walls fade away and domains and walls become indistinguishable. The latter process transforms the structure into a planar vortex which is the charge-free magnetization pattern. Hence a continuous reorientation transition through the phase of canted domains occurs. In this region K_2 has a strong influence on the microstructure of magnetization.

The third possible path for the reorientation of the magnetization proceeds via the forth quadrant of the anisotropy space ($K_1^{eff}>0, K_2<0$). In this region (inset *coexistence* in Fig. 1) we find that the average vertical component of magnetization goes gradually from almost unity above $K_2=-\frac{1}{2}K_1^{eff}$ to zero at $K_1^{eff}=0$. This continuous change of the magnetization component can lead to the erroneous conclusion that the reorientation proceeds via the canting of magnetization. The canting phase, however, does not exist in this part of the anisotropy space.[11,15] In the simulation we find a magnetic microstructure that consists of domains magnetized perpendicular and in plane, i.e., a coexistence of the two phases [histogram, Fig. 4(b)]. Hence the very existence of two local minima in the free energy[11] leads to the appearance of domains with vertical and in-plane orientations of the magnetization. The borderlines of the phase of coexisting domains in the calculations are in good agreement with the experimentally defined borders of the ''gray'' zone of SRT in Co/Au(111).[4] The first experimental manifestation of coexisting domains in Co/Au(111)/W(110) was published recently.[7]

In our simulation we find that the magnetic transition is continuous. Our results rule out the models discussed in literature for $T=0$ K, i.e., the ''perfect delay'' and the ''Maxwell'' convention.[14] A typical microstructure of a state of coexistence phases and the frequency distribution of the vertical component of magnetization for that state are presented in Fig. 4. The histogram [Fig. 4(b)] demonstrates that the majority of the magnetic moments build an angle of either 0 or $\pm\pi/2$ with the film normal, i.e., vertical and in-plane magnetized domains are formed. The domain walls cause a small amount of moments with deviating orientations. The depths of the local minima of the free energy depend on the values of K_1^{eff} and K_2.[11] In our simulations we find an increase/decrease of the in-plane/vertical domains size with

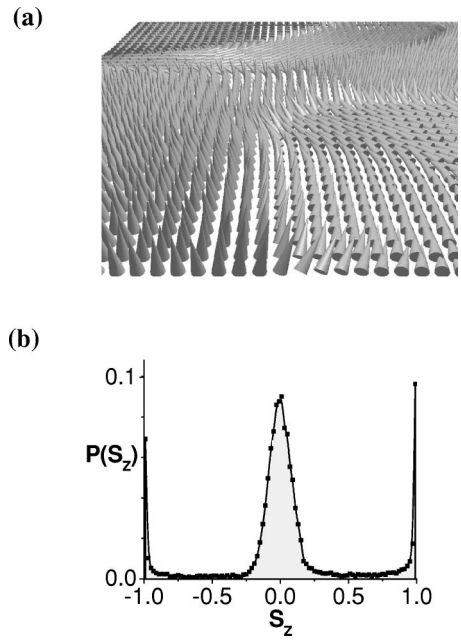

FIG. 4. Microstructure of the state of coexisting phases for $K_1^{eff}=E_D$, $K_2=-0.8E_D$, and $k_BT/J=0.05$. (a) Perspective view of an enlarged part of the sample. For clarity only one row out of two and one moment out of two in the row are drawn as cones. (b) Frequency distribution of the magnetization orientation. The population frequency is given as a function of the magnetization component along the normal. The plot is generated from the simulation shown in *a*.

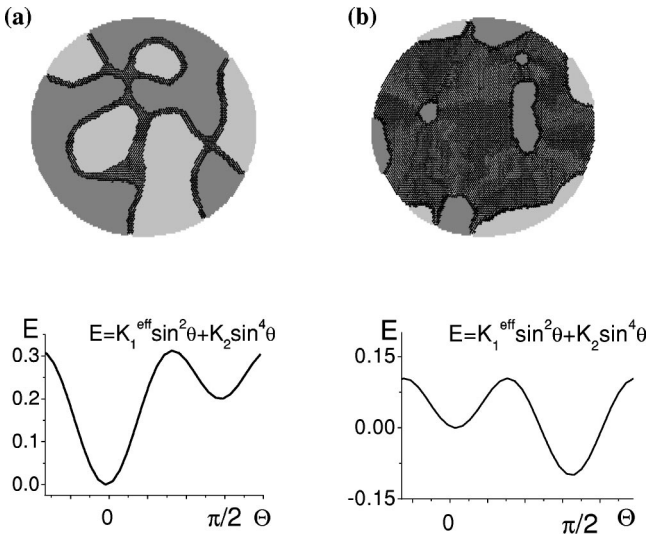

FIG. 5. Top view of the microstructure of the state of coexisting phases and corresponding energetic potential. Dark- and light-gray areas represent spin-up and -down domains correspondingly. Black arrows show the in-plane domains, $k_BT/J=0.05$. In (a) The situation of a deeper minimum for the vertical phase ($K_2=-0.8K_1^{eff}$) is shown. The region between the vertical domains are in-plane magnetized domains. (b) Exhibits the microstructure for the situation that the energy minimum for the in-plane phase is deeper ($K_2=-1.1K_1^{eff}$). Note that vertical domains remain at the edges and in the center of domains with ''rotating'' in-plane magnetization. They will shrink to the center of vortices found in the in-plane phase.

decreasing K_1^{eff}. This means that the frequencies of population of the two phases of the magnetization depend on the ratio K_1^{eff}/K_2.

A top view of the microstructures of the state of coexisting phases is presented in Fig. 5. Figure 5(a) represents the situation where the vertical magnetization is favored, which leads to the preponderance of vertically magnetized domains. On a first glance the in-plane domains could be misleadingly interpreted as walls. The magnetization profile, however, deviates completely from that of a domain wall. While in the wall a continuous tilting of the magnetization is expected, we find that all spins lie in the film plane except for a thin region, i.e., a wall, along the domain contours [Fig. 5(a)]. The walls are not exactly described in our simulations as the mesh size is too large. If the in-plane orientation is more favorable (deeper minimum) an in-plane vortex-like structure appears [Fig. 5(b)]. The vortex-structure is a consequence of the minimization of the magnetostatic energy as no in-plane anisotropy is assumed. The vertical domains remain in the core of the vortices and at the sample edges. Again a continuous transition between adjacent phases is achieved via the microstructure.

We have explored the population of the different states of the coexisting phases as a function of time and size of the sample. The relative population of the in-plane and vertical magnetizations persists for every relaxation process for a given geometry. The spatial arrangement of the vertical and in-plane domains, however, can change with time, i.e., the number of Monte Carlo steps. This means that snapshots of the equilibrium microstructure can differ during the same Monte Carlo procedure. Different spatial arrangements of domains also depend on the starting conditions for identical relaxation procedures.

The multidomain state of the coexisting phase transforms into a single domain state when the sample size is smaller than the typical domain size for a given K_1^{eff}/K_2. In that situation the ratio of K_1^{eff}/K_2 defines the probability to find the sample in a vertical or an in-plane magnetized single domain state. Domains with an in-plane magnetization do not show a vortex structure in small samples. The monodomain configuration is energetically preferred as the gain in the dipolar energy is lower than the loss in the exchange energy for small structures.[21]

In conclusion, a strong influence of the second-order perpendicular anisotropy on the microstructure of the spin reorientation transition is found. For $K_2>0$ a transition via a canted domain structure is established that yields a smooth, continuous connection between the vertical domain structure and the vortex structure with in-plane magnetization. For $K_2<0$ a continuous reorientation via a state of coexisting vertical and in-plane magnetized domains occurs. The sizes of the vertical and the in-plane domains depend on the ratio of K_1^{eff} and K_2. The spatial arrangement of the domains can change with time, while the frequency distribution of the in-plane and the vertical phases is invariable.

*Corresponding author. Email address: vedmedenko@physnet.uni-hamburg.de

[1] D. P. Pappas, K.-P. Kämper, and H. Hopster, Phys. Rev. Lett. **64**, 3179 (1990).
[2] R. Allenspach and A. Bischof, Phys. Rev. Lett. **69**, 3385 (1992).
[3] H. P. Oepen, Y. T. Millev, and J. Kirschner, J. Appl. Phys. **81**, 5044 (1997).
[4] H. P. Oepen, M. Speckmann, Y. T. Millev, and J. Kirschner, Phys. Rev. B **55**, 2752 (1977).
[5] M. Speckmann, H. P. Oepen, and H. Ibach, Phys. Rev. Lett. **75**, 2035 (1995).
[6] M. Farle, W. Platow, A. N. Anisimov, B. Schulz, and K. Baberschke, J. Magn. Magn. Mater. **165**, 74 (1997).
[7] T. Duden and E. Bauer, in *Magnetic Ultrathin Films, Multilayers and Surfaces*, edited by J. Tobin, D. Chambliss, D. Kubinski, K. Barmak, P. Dederichs, W. de Jonge, T. Katayama, and A. Schuhl, MRS Symposia Proceedings No. 475 (Materials Research Society, Pittsburgh, 1997), p. 273.
[8] Y. Yafet and E. M. Gyorgy, Phys. Rev. B **38**, 9145 (1988).
[9] A. B. MacIsaac, K. De'Bell, and J. P. Whitehead, Phys. Rev. Lett. **80**, 616 (1998); K. De'Bell, A. B. MacIsaac, I. N. Booth, and J. P. Whitehead, Phys. Rev. B **55**, 15 108 (1997).
[10] E. Y. Vedmedenko, H. P. Oepen, A. Ghazali, J.-C.S. Lévy, and J. Kirschner, Phys. Rev. Lett. **84**, 5884 (2000).
[11] H. B. G. Casimir, J. Smit, U. Enz, J. F. Fast, H. P. J. Wijn, E. W. Gorter, A. J. W. Duyvesteyn, J. D. Fast, and J. de Jong, J. Phys. Radium **20**, 360 (1959).
[12] C. Chappert and P. Bruno, J. Appl. Phys. **64**, 5736 (1988).
[13] H. Fritzsche, J. Kohlhepp, and U. Gradmann, J. Magn. Magn. Mater. **148**, 154 (1995).
[14] S. Nieber and H. Kronmüller, Phys. Status Solidi B **165**, 503 (1991).
[15] Y. Millev and J. Kirschner, Phys. Rev. B **54**, 4137 (1996).
[16] E. Y. Vedmedenko, A. Ghazali, and J-C. S. Lévy, Phys. Rev. B **59**, 3329 (1999).
[17] H. Träuble, O. Boser, H. Kronmüller, and A. Seger, Phys. Status Solidi **10**, 283 (1965).
[18] P. J. Jensen and K. H. Bennemann, Phys. Rev. B **52**, 16 012 (1995); K. Baberschke and M. Farle, J. Appl. Phys. **81**, 5038 (1997).
[19] R. Allenspach, J. Magn. Magn. Mater. **129**, 160 (1994).
[20] J.-C. S. Lévy, Phys. Rev. B **63**, 104409 (2001).
[21] W.F. Brown, in *Selected Topics in Solid State Physics*, edited by E. P. Wohlfarth (North-Holland, Amsterdam, 1962), Vol. I.